Carbohydrate Research, 170 (1987) 167–179
Elsevier Science Publishers B.V., Amsterdam – Printed in The Netherlands

STRUCTURAL ANALYSIS OF TWO 2-DEOXY ANALOGUES OF α- AND β-KDO AND THE METHYL α- AND β-GLYCOSIDES OF KDO, AND DETERMINATION OF THEIR METAL-ION-BINDING PROPERTIES

KRISTINA LUTHMAN, ALF CLAESSON,

Department of Organic Pharmaceutical Chemistry, Uppsala Biomedical Center, Uppsala University, P.O. Box 574, S-751 23 Uppsala (Sweden)

LENNART KENNE,

Department of Organic Chemistry, Arrhenius Laboratory, University of Stockholm, S-106 91 Stockholm (Sweden)

AND INGEBORG CSÖREGH

Department of Structural Chemistry, Arrhenius Laboratory, University of Stockholm, S-106 91 Stockholm (Sweden)

(Received March 23rd, 1987; accepted for publication, June 15th, 1987)

ABSTRACT

Ammonium 2,6-anhydro-3-deoxy-D-*glycero*-D-*talo*-octonate (**1**), a potent inhibitor of the enzyme CMP-KDO synthetase, its C-2 epimer **2**, and the methyl β- (**3**) and α-glycoside (**4**) of KDO were studied by ^{1}H- and ^{13}C-n.m.r. spectroscopy. Compound **1** was also analysed by X-ray crystallography. Each compound adopted a $^5C_2$ chair conformation with the side chain equatorial. The preponderant side-chain conformation of **1** in solution was the same as that in the crystal and was stabilised by an intramolecular hydrogen bond from HO-8 to the carboxylate group. This hydrogen bond appeared to be present also in **3**. However, the side-chain conformation of **2** and **4** was different from that in **1** and **3**. The metal-ion-binding properties, determined on the basis of the line-broadening effects of Mn^{2+} on the ^{13}C-n.m.r. signals, showed that the carboxylate group was involved in the binding with O-8 in **1** and **3** and with O-6 and O-8 in **2** and **4**.

INTRODUCTION

Ammonium 2,6-anhydro-3-deoxy-D-*glycero*-D-*talo*-octonate (**1**), the 2-deoxy analogue of 3-deoxy-β-D-*manno*-2-octulosonic acid (KDO), is a potent inhibitor (K_i 3.9 μM) of the enzyme CTP:3-deoxy-D-*manno*-octulosonate cytidylyltransferase (CMP-KDO-synthetase, EC 2.7.7.38), which catalyses the conversion of KDO into its CMP derivative[1]. The enzyme is unique to Gram-negative bacteria where it is involved in the biosynthesis of lipopolysaccharides[2,3] (LPS). These macromolecular structures, which are of crucial importance to the viability of the bacteria, are

0008-6215/87/$ 03.50

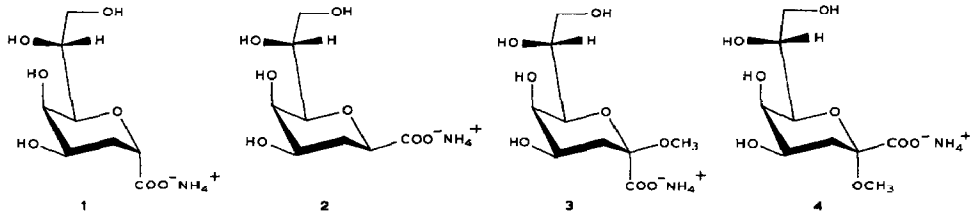

1 2 3 4

attractive targets for chemotherapy. Whereas **1** is a strong inhibitor, its C-2 epimer (**2**) is inactive. In order to probe the fine structure of this prototypical enzyme inhibitor and its epimer, we have applied ^{1}H- and ^{13}C-n.m.r. spectroscopy and compared the results for **1** with those obtained by X-ray crystallography.

In addition to being a constituent of LPS, KDO is also found in the capsular polysaccharides of some Gram-negative bacteria[4]. N.m.r. data have shown KDO to be α in LPS[5–7] and both α and β in the capsular polysaccharides[8–12]. KDO residues in LPS are expected to participate in binding of the Mg^{2+} and Ca^{2+} ions known to surround the negatively charged surface of Gram-negative bacteria. Strain *et al.*[13] studied the metal-ion binding properties of the phosphate groups in LPS from two mutants of *E. coli* by ^{31}P-n.m.r. spectroscopy. It was not possible to determine if KDO participated in the metal-ion-binding because of the complexity of the ^{13}C-n.m.r. spectra obtained from complete LPS. In order to determine if and how KDO interacts with divalent metal ions, the methyl β- (**3**) and α-glycoside (**4**) of KDO have been used as model compounds for the binding of the paramagnetic ion Mn^{2+}, as were the 2-deoxy analogues **1** and **2**.

EXPERIMENTAL

Compounds **1–4** were synthesised from the glycosyl chloride of 4,5,7,8-tetra-*O*-acetyl-KDO by methods described in the literature[1,12,14] and isolated as the ammonium salts.

Crystallography. — Compound **1** crystallised from aqueous 2-propanol as a monohydrate ($C_8H_{19}NO_8$). A crystal with the approximate dimensions 0.62 × 0.48 × 0.40 mm was selected for data collection. The intensities of 1253 reflections with $\theta < 67°$ were measured on a Philips PW 1100 computer-controlled diffractometer at room temperature, with graphite-monochromated Cu-$K\alpha$ radiation and the $\omega - 2\theta$ scan technique. The net intensities were corrected for Lorentz and polarisation effects, but the rather low absorption effect ($\mu_{x\text{-ray,calc.}} = 10.7\ cm^{-1}$) was neglected. The unit cell is pseudo-tetragonal with $a = b = 11.925(2)$ Å and $c = 8.401(2)$ Å, and with four formula units in the cell. The space-group symmetry is, however, orthorhombic, $P2_12_12_1$. The cell dimensions were refined by least-squares fitting of the preliminary cell parameters, measured on the diffractometer, to powder data from a Guinier photograph taken with strictly monochromated Cu-$K\alpha_1$ radiation ($\lambda = 1.5406$ Å) and using Si ($a = 5.4309$ Å at 298 K) as an

TABLE I

FRACTIONAL ATOMIC PARAMETERS ($\times 10^4$) AND EQUIVALENT ISOTROPIC TEMPERATURE FACTORS ($\times 10^3$) FOR THE NON-HYDROGEN ATOMS, AND FRACTIONAL ATOMIC COORDINATES ($\times 10^3$) AND GROUP ISOTROPIC TEMPERATURE FACTOR ($\times 10^3$) FOR THE HYDROGENS INVOLVED IN HYDROGEN BONDS[a]

Atom	X	Y	Z	U_{eq}/U (Å^2) [b]
O-6	2775(2)	1333(2)	6509(3)	29(1)
C-2	1896(3)	758(3)	7342(5)	31(1)
C-1	838(3)	633(3)	6293(5)	32(1)
O-10	−28(2)	267(2)	6927(3)	40(1)
O-11	943(2)	845(2)	4831(3)	39(1)
C-3	1713(4)	1258(3)	8996(5)	36(1)
C-4	1593(4)	2530(3)	8935(5)	36(1)
O-4	1532(3)	3007(3)	10482(3)	49(1)
C-5	2556(3)	3052(3)	7990(5)	33(1)
O-5	3605(2)	2830(2)	8750(4)	42(1)
C-6	2563(3)	2509(3)	6350(5)	28(1)
C-7	3443(3)	2956(3)	5220(5)	32(1)
O-7	3146(2)	4093(2)	4908(4)	43(1)
C-8	3515(4)	2256(4)	3702(5)	40(1)
O-8	2446(3)	2017(3)	3019(3)	47(1)
O-W	1001(2)	5037(3)	15097(4)	44(1)
N	−2(3)	4258(3)	12153(4)	38(1)
H-O4	189	281	1103	99(7)
H-O5	377	347	930	99(7)
H-O7	359	435	442	99(7)
H-O8	183	186	356	99(7)
H-W1	156	480	1506	99(7)
H-W2	94	514	1597	99(7)
H-N1	47	354	1170	99(7)
H-N2	−65	354	1205	99(7)
H-N3	−18	493	1145	99(7)
H-N4	43	456	1318	99(7)

[a] Positions of hydrogen atoms are taken from difference Fourier calculations and are not refined. E.s.d. values are given in parentheses. The atoms are numbered according to Fig. 1.

[b] $U_{eq} = \frac{1}{3}\Sigma_i\Sigma_j U_{ij}\,\mathbf{a}^*_i\mathbf{a}^*_j\,a_i a_j$.

internal standard. In the refinement, 38 observed line positions with $12° < 2\theta < 55°$ were used. Direct methods using the MULTAN program system[15] gave a reasonable model with fourteen atoms out of the seventeen non-hydrogen atoms of the structure, which was completed and refined using the SHELX program system[16]. The positions of the hydrogens connected to carbons were generated after each cycle of the refinement using geometrical evidence. The hydrogens attached to oxygen and nitrogen were located from difference Fourier maps and kept fixed during the subsequent calculations.

In the last refinement, the positions of the non-hydrogen atoms were refined together with their anisotropic temperature factors. Two group isotropic temperature factors were refined for the calculated hydrogens and for the remainder, respectively. The refinement of the structural model against 1189 structure factors,

TABLE II

INTRAMOLECULAR BOND LENGTHS (IN Å) AND BOND ANGLES (IN °) INVOLVING THE NON-HYDROGEN ATOMS[a]

Distances			
O-6-C-2	1.435(4)	C-5-C-6	1.522(6)
C-2-C-3	1.528(6)	C-6-O-6	1.431(4)
C-2-C-1	1.546(5)	C-6-C-7	1.513(6)
C-3-C-4	1.525(6)	C-7-O-7	1.426(5)
C-4-O-4	1.420(5)	C-7-C-8	1.526(6)
C-4-C-5	1.529(6)	C-8-O-8	1.427(5)
C-5-O-5	1.430(5)	C-1-O-10	1.241(5)
		C-1-O-11	1.260(5)
Angles			
C-6-O-6-C-2	112.6(3)	C-5-C-6-O-6	109.5(3)
O-6-C-2-C-1	111.3(3)	C-5-C-6-C-7	115.0(3)
O-6-C-2-C-3	111.2(3)	O-6-C-6-C-7	106.3(3)
C-3-C-2-C-1	116.0(3)	C-6-C-7-C-8	111.7(3)
C-2-C-3-C-4	111.8(3)	C-6-C-7-O-7	106.2(3)
C-3-C-4-C-5	110.6(3)	O-7-C-7-C-8	112.4(3)
C-3-C-4-O-4	111.9(3)	C-7-C-8-O-8	113.3(3)
O-4-C-4-C-5	110.5(3)	C-2-C-1-O-11	117.1(3)
C-4-C-5-C-6	107.5(3)	C-2-C-1-O-10	117.9(3)
C-4-C-5-O-5	110.5(3)	O-10-C-1-O-11	124.8(3)
O-5-C-5-C-6	108.7(3)		

[a] E.s.d. values are given in parentheses. The atoms are numbered according to Fig. 1.

all with $F > 6\sigma(F)$ and unit weights, converged to a final R value of 0.0448. Eighteen reflections ($\theta_{max} < 20°$) had considerably weaker observed structure factors than those calculated, probably depending on extinction, and were excluded from the last refinement.

The fractional atomic parameters for the non-hydrogen atoms and for the hydrogens involved in the hydrogen bonds are listed in Table I.

N.m.r. spectroscopy. — Spectra were recorded for ~0.2M (20 mg/0.5 mL) solutions in D_2O in 5-mm diameter tubes between 25° and 85° with a JEOL GX-400 spectrometer operating at 400 (^1H) and 100 MHz (^{13}C). Chemical shifts are reported in p.p.m. using 1,4-dioxane (δ 67.40, ^{13}C) and sodium 3-trimethylsilylpropanoate-d_4 (^1H) as internal references. ^1H-N.m.r. data were obtained by 1D and 2D spectroscopy (JRES, COSY, NOESY) from which the assignments of the signals could be made. The coupling constants were measured directly from the spectra with the assumption that the first-order coupling approximation was valid.

^{13}C-N.m.r. signals were assigned by differential isotope shifts[17] (DIS), which were obtained for solutions in D_2O and H_2O containing 5% of D_2O, respectively, and by C–H chemical-shift correlation 2D-spectroscopy.

Effects of temperature on the ^{13}C chemical shifts were measured at 15° intervals from 25° to 85° for solutions in D_2O (internal 1,4-dioxane, δ 67.40).

Metal-ion-interaction experiments were performed on solutions in D_2O con-

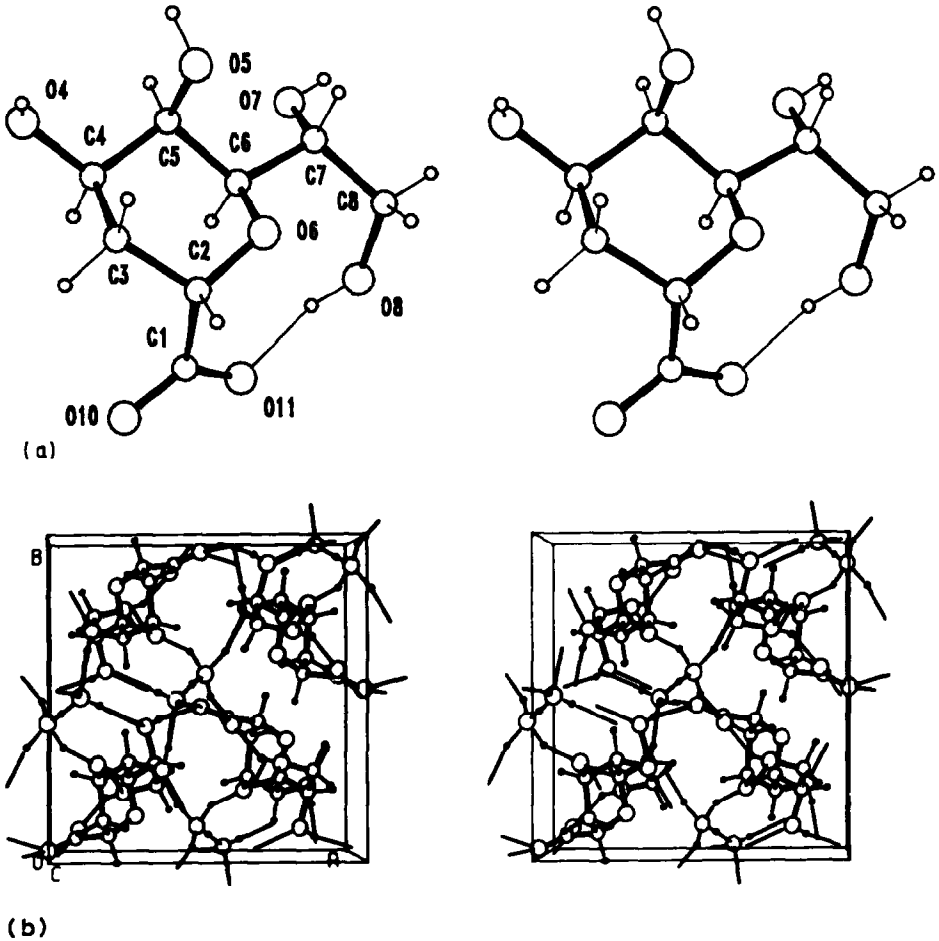

Fig. 1. (*a*) Stereographic drawing of the molecular structure of the 2,6-anhydro-3-deoxy-D-*glycero*-D-*talo*-octonate anion; (*b*) stereoscopic packing illustration of the crystal structure.

taining 100 μmol of glycoside and 4.5 and 9 μmol of $MnCl_2 \cdot 4H_2O$, respectively.

RESULTS AND DISCUSSION

X-Ray crystallography. — As shown in Fig. 1, the pyranose ring of **1** exists in a $^5C_2$ chair conformation [the r.m.s. torsion angle is 57.14°; the calculated ring-puckering parameters[18] are $\theta = 8.4\ (4)°$ and $\phi = -78(2)°$]. The carboxylate group and O-5 are axial, whereas O-4 and the side chain are equatorial. The conformation of the side chain is stabilised by an intramolecular hydrogen bond from O-8 to O-11. The observed values of bond lengths and bond angles generally conform to the expected values (Table II).

The crystal structure shows a hydrogen-bonded network of carbohydrate

TABLE III

HYDROGEN BOND DISTANCES AND ANGLES[a]

Contact	*Donor-H* (Å)	*H···Acceptor* (Å)	*Donor···Acceptor* (Å)	*Donor-H···Acceptor* (°)
O-8-H·····O-11 (a)[b]	0.89	1.93	2.736(4)	151
N-1-H·····O-4 (a)	1.09	1.75	2.747(5)	150
N-4-H·····O-W (a)	1.07	1.83	2.900(5)	172
O-7-H·····O-10 (b)	0.74	2.05	2.775(4)	168
O-4-H·····O-8 (c)	0.67	2.03	2.669(4)	159
OW-1-H·····O-7 (c)	0.73	2.07	2.800(4)	178
O-5-H·····O-W (d)	0.91	1.92	2.823(4)	169
OW-2-H·····O-10 (e)	0.75	2.08	2.769(4)	154
N-2-H·····O-5 (f)	1.16	1.97	3.088(5)	160
N-3-H·····O-11 (g)	1.02	1.78	2.760(4)	160

[a] Positions of hydrogens are taken from difference electron density calculations and are not refined. E.s.d. values are given in parentheses. The atoms are numbered according to Fig. 1. [b] Symmetry operations: a, x,y,z; b, $0.5+x,0.5-y,1-z$; c, $x,y,1+z$; d, $0.5-x,1-y,-0.5+z$; e, $-x,0.5+y,2.5-z$; f, $-0.5+x,0.5-y,2-z$; g, $-x,0.5+y,1.5-z$.

TABLE IV

^{1}H-N.M.R. DATA[a] FOR COMPOUNDS 1–4 OBTAINED AT 40°.

Compound	*H-2*	*H-3a*	*H-3e*	*H-4*	*H-5*	*H-6*	*H-7*	*H-8*	*H-8'*	*OCH$_3$*
1	4.35	2.03	2.22	3.74	3.99	3.57	3.84	3.8[b]	3.8[b]	
2	3.89	1.70	2.05	3.90	3.98	3.39	3.89	3.84	3.70	
3		1.78	2.40	3.76	3.97	3.65	3.94	3.90	3.77	3.32
4		1.79	2.03	4.04	4.02	3.56	3.96	3.95	3.68	3.16

	$J_{2,3a}$	$J_{2,3e}$	$J_{3a,3e}$	$J_{3a,4}$	$J_{3e,4}$	$J_{3e,5}$	$J_{4,5}$	$J_{5,6}$	$J_{6,7}$	$J_{7,8}$	$J_{7,8'}$	$J_{8,8'}$
1	6.7	2.1	−12.4	12.4	5.0	1.0	3.2	1.4	8.4	4.6	2.2	N.d.[c]
2	12.2	2.5	−12.2	12.2	5.0	1.0	3.0	0.8	8.4	3.0	5.7	−11.8
3			−12.4	12.4	4.8	1.0	3.0	1.2	8.9	4.5	2.1	−12.0
4			−12.3	12.3	5.2	0.9	3.1	0.7	8.8	3.0	7.0	−12.3

[a] Chemical shifts (δ in p.p.m.; internal sodium 3-trimethylsilylpropanoate-d_4), J in Hz. [b] Overlapping signals. [c] Not determined.

anions, ammonium cations, and water molecules. All hydrogens which belong to oxygen or nitrogen take part in hydrogen bonding, and the bond distances and bond angles are listed in Table III.

The conformation of the side chain found in the crystal structure was compared with that found in solution and is discussed below.

^{1}H-N.m.r. data. — Spectra were obtained at 40°. Chemical shifts and coupling constants for **1–4** are presented in Table IV. Due to the complexity of the spectra, 2D techniques (JRES, COSY, NOESY) were used for assignments. Each compound adopted the $^5C_2$ chair conformation as evident from the coupling constants.

The configuration at C-2 in **1** and **2** was determined by analysis of the J values for H-3*e* and H-3*a* (Fig. 2). The $J_{2,3a}$ value of 6.7 Hz for **1** indicated a *gauche* relation, whereas the corresponding value (12.2 Hz) for **2** indicated a *trans*-diaxial relation. The $J_{2,3e}$ values were 2.1 and 2.5 Hz, respectively.

The differences in chemical shifts of the signals for H-3*a* and H-3*e* for KDO derivatives can be used to assign anomeric configurations[19]. Thus, the resonance of H-3*e* in a β anomer should appear more downfield than the corresponding signal in an α anomer, as also found for **1** and **2**. However, a greater difference in chemical shift was observed for **2** than for **1**, in contrast to the findings for **3** and **4**. Introduction of an axial MeO at C-2, as in **4**, influences only the chemical shift of the signal for H-3*a* by +0.1 p.p.m., whereas introduction of an equatorial MeO group, as in **3**, influences that for H-3*e* by +0.2 and H-3*a* by −0.25 p.p.m., respectively.

The preponderant conformation of the side chain of **1** in solution was similar to the conformation found in the crystal. The $J_{6,7}$ value of 8.4 Hz is in agreement with a preponderant *trans* relationship of H-6,7 (Fig. 1). Other rotamers about the

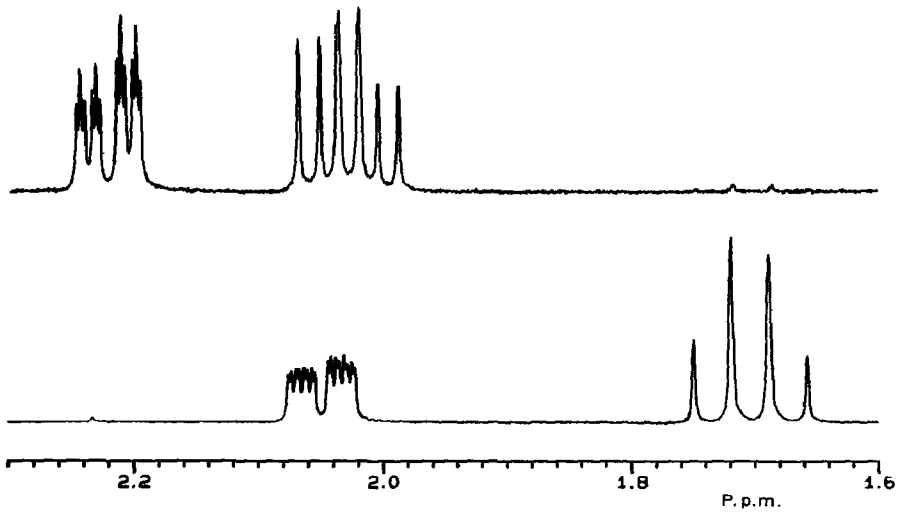

Fig. 2. The 400-MHz ^{1}H-n.m.r. spectra of the deoxyproton region for 1 and 2.

C-6–C-7 bond appear unlikely because of considerable *syn* interactions of the substituents at C-7 and HO-5*a*.

The molecular structure shows an intramolecular hydrogen bond between the carboxylate group and HO-8 (Fig. 1). The $J_{7,8}$ and $J_{7,8'}$ values of 4.6 and 2.2 Hz, respectively, indicate a high population of the conformation in which HO-7,8 are *gauche*, a conformation stabilised by the "*gauche* effect". In this conformation, HO-8 is turned towards the carboxylate group to facilitate the formation of the proposed hydrogen bond. A hydrogen bond in the analogous position has been proposed by Bhattacharjee *et al.*[12] for β-glycosides of KDO in capsular polysaccharides. The side-chain conformation in **3** appears to be similar to that in **1** since the relevant *J* values are similar (Table IV). Similar studies of the side-chain conformation have been reported by Birnbaum *et al.*[20].

^{13}C-N.m.r. data. — The spectra were obtained at 40° and the chemical shifts are presented in Table V. The ^{13}C signals of **1** and **2** were initially assigned by

TABLE V

^{13}C-N.M.R. DATA[a] FOR COMPOUNDS 1–4 OBTAINED AT 40°

Compound	*C-1*	*C-2*	*C-3*	*C-4*	*C-5*	*C-6*	*C-7*	*C-8*	*OMe*
1	179.06	74.99	29.42	67.72	67.38	74.66	70.15	64.82	
2	178.87	77.51	32.17	70.13	67.53	77.91	70.59	64.04	
3	174.40	102.11	35.27	68.30	66.28	74.31	70.01	64.86	52.28
4	176.03	101.32	34.93	66.83	67.18	72.30	70.23	63.94	51.42

[a] Chemical shifts [δ in p.p.m.; internal 1,4-dioxane (δ 67.40)].

TABLE VI

EFFECTS OF TEMPERATURE ON CHEMICAL SHIFTS[a] OF THE ^{13}C RESONANCES FOR COMPOUNDS 1–4

Compound	*δ 85° − δ 25° (p.p.m.)*								
	C-1	*C-2*	*C-3*	*C-4*	*C-5*	*C-6*	*C-7*	*C-8*	*OCH_3*
1	−0.38	0.09	0.16	0	0.33	0.05	0.41	0	
2	−0.50	0.34	0.15	0.10	0.27	0.43	0.38	0.21	
3	−0.40	0.21	−0.05	0.14	0.46	0.23	0.45	0	−0.13
4	−0.68	0.14	0.20	0.17	0.34	0.44	0.55	0.30	0

[a] Relative to that of internal 1,4-dioxane (δ 67.40).

differential isotope shift (DIS) experiments[17] and C–H chemical-shift correlation 2D spectroscopy.

The assignments for **3** and **4** agreed with those reported[11,12]. In order to verify the assignments for **1** and **2**, 2D CH-correlation experiments were performed which showed identical results. The chemical shifts of almost all of the ^{13}C resonances were temperature-dependent in the range 25–85° for solutions in D_2O. The chemical shift differences ranged from −0.68 to 0.55 p.p.m. (Table VI), with C-1,5,7 showing the largest differences and C-3,4,8 the smallest. Especially pronounced differences were found for C-8 in the β-anomers **1** and **3**. All the shift variations were downfield except that of the resonance for C-1 in each of the four compounds. The signals for C-3 and MeO in **3** were shifted upfield with increase in temperature.

There is confusion[5,11,12] about the assignments of the signals of C-4 and C-5 in **4**. For unambiguous assignments, long-range CH-correlation experiments were performed, which showed the signals at δ 66.83 and 67.18 to be associated with C-4 and C-5, respectively. The chemical shift for the resonance of C-4 was much less temperature-dependent than for C-5, which also accorded with the assignments made (Table VI).

The intramolecular hydrogen bond between the carboxylate group and HO-8 in **1** (Fig. 1) could also be detected in ^{13}C-n.m.r. spectra. The chemical shift difference (~0.9 p.p.m.) between the resonances for C-8 in **3** and **4** was reported[12] to be an indication of a hydrogen bond in the β-glycoside **3**. The chemical shift difference for the resonances of C-8 in **1** and **2** was 0.8 p.p.m. and could also be explained by the formation of a hydrogen bond. In addition, the temperature dependence of the chemical shifts of the resonances for C-8 was different for **1** and **3** compared to **2** and **4** which further confirmed different conformations around the C-7–C-8 bond. At higher temperatures, rotation around the C-7–C-8 bond will increase. The conformations will then approach similar population distributions in **1** and **3** as in **2** and **4**, which will change the chemical shift of the resonance of C-8 towards the same value.

The spin–lattice relaxation times (T_1) can be used to demonstrate hindered rotation in a molecule. It can be expected that rotation of the side chain in **1** will be

TABLE VII

SPIN–LATTICE RELAXATION TIMES, T_1 (s) FOR COMPOUNDS 1 AND 2

Compound	*C-2*	*C-3*	*C-4*	*C-5*	*C-6*	*C-7*	*C-8*
1	1.2	0.6	1.2	1.1	1.2	1.2	0.8
2	0.9	0.5	0.9	0.8	0.9	0.9	0.6

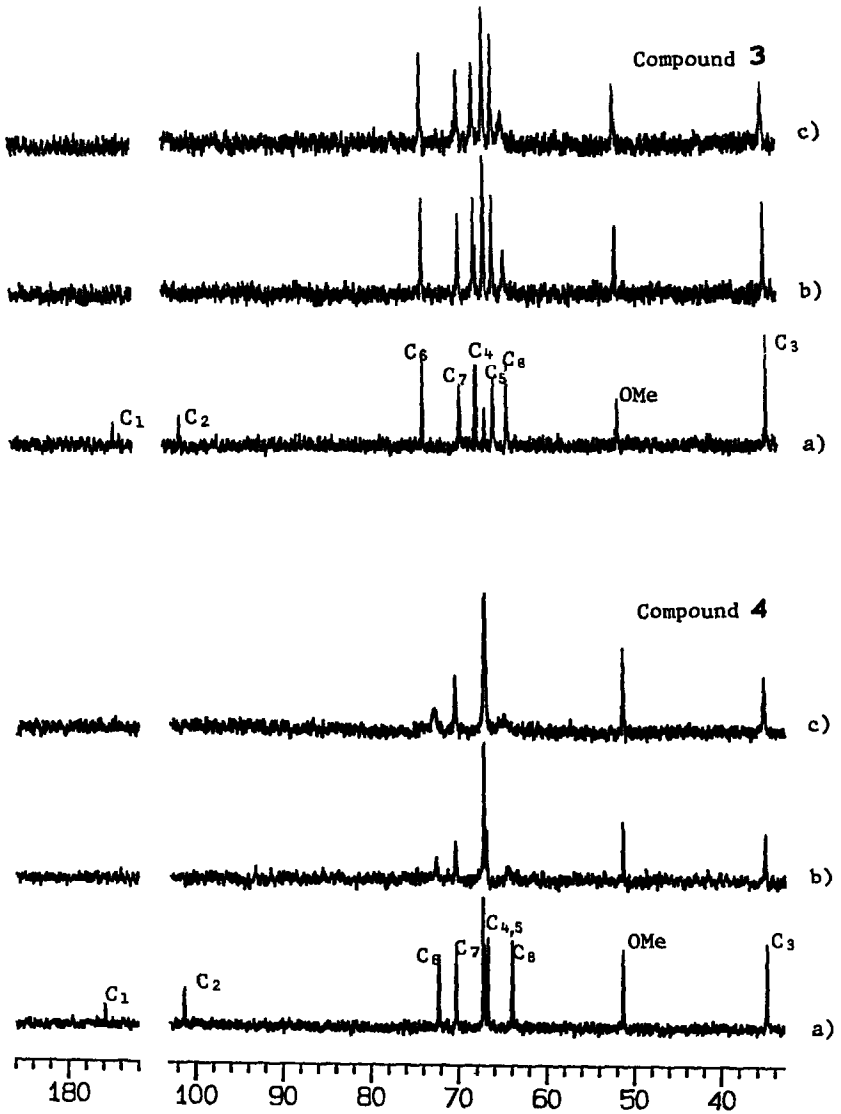

Fig. 3. Proton-decoupled ^{13}C-n.m.r. spectra of solutions containing 100 μmol of the methyl β- (3) and α-glycoside (4) of KDO in 0.4 mL of D_2O; (*a*) without Mn^{2+}, and in the presence of (*b*) 4.5 and (*c*) 9 μmol of Mn^{2+}.

restricted due to the intramolecular hydrogen bond. The relative sizes of T_1 for carbons in the side chain compared to those of the carbons in the pyranose ring are similar in both **1** and **2**, which indicates that there was no major difference in rotational freedom (Table VII).

Metal-ion interactions. — Divalent cations are bound in high concentration to the surface of Gram-negative bacteria, and the phosphate groups and KDO residues

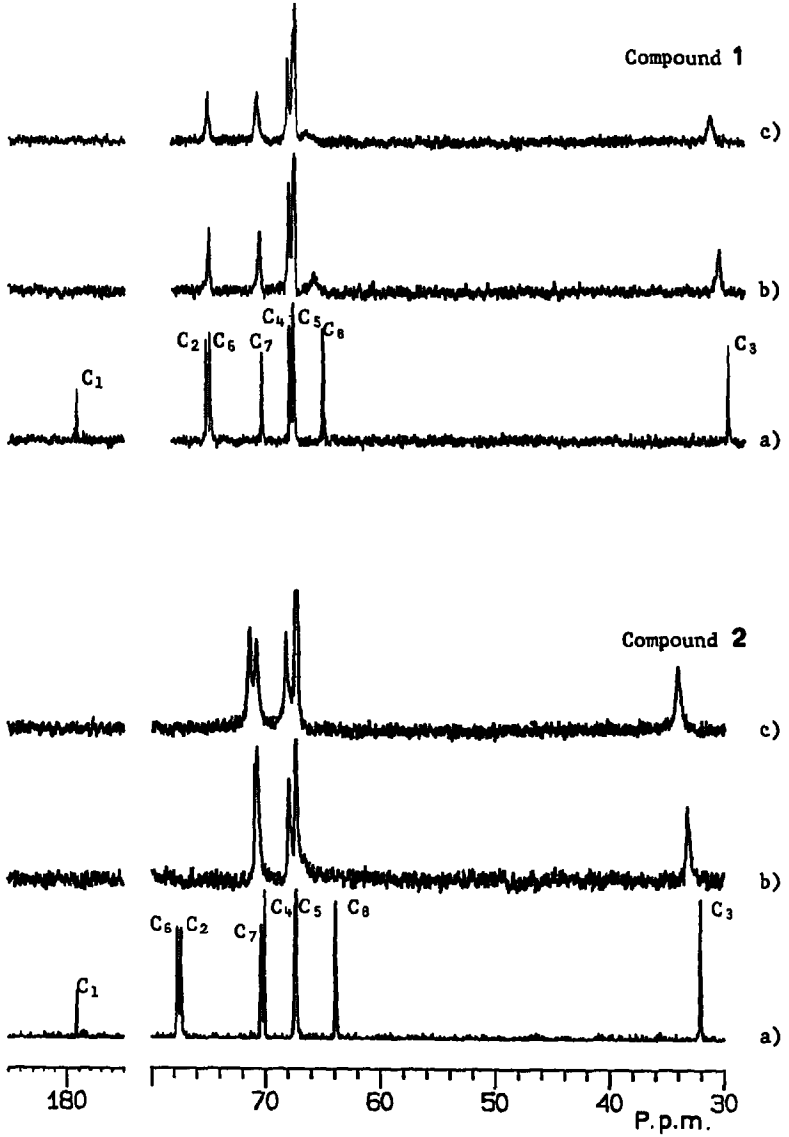

Fig. 4. Proton-decoupled ^{13}C-n.m.r. spectra of solutions containing 100 μmol of 2-deoxy-β- (**1**) or -α-KDO (**2**) in 0.4 mL of D_2O: (*a*) without Mn^{2+}, and in the presence of (*b*) 4.5 and (*c*) 9 μmol of Mn^{2+}.

in LPS are thought to be the binding sites. The paramagnetic ion Mn^{2+} is often used in biological studies instead of Mg^{2+}, since only traces are needed in order to permit observations of specific line-broadening if binding occurs. The resonances of carbons near the binding site(s) would be expected to broaden significantly more than other resonances.

Studies by Daman *et al.*[21] of the interactions of Mn^{2+} and Gd^{3+} with *N*-acetylneuraminic acid revealed multiple binding sites for Mn^{2+}, one near the carboxyl moiety and at least one near the side chain and NAc-5. However, Gd^{3+} was thought to bind to one site involving the carboxyl group and C-8,9 in the side chain.

The effect of the addition of Mn^{2+} on the ^{13}C-n.m.r. spectra of **1**–**4** is shown in Figs. 3 and 4. The resonances attributed to C-1 and C-2 of **4** disappeared immediately, whereas that of C-8 was broadened considerably (Fig. 3). In addition, the C-6 resonance was shifted downfield and broadened. Further addition of Mn^{2+} resulted in complete disappearance of the C-8 signal and extensive broadening of the C-6 resonance. Thus, the primary binding site appears to involve the carboxylate group, the ring oxygen, and C-8. This result suggested a higher population of the *trans*-rotamer of the C-7–C-8 bond, since HO-8 will occupy a position close to the ring oxygen in order to facilitate the ion binding.

Also, in **2**, the primary binding site involves C-1, the ring oxygen, and C-8 (Fig. 4). However, the C-3 resonance in **2** appeared to be more affected than in **4**, with a larger downfield shift and extensive line broadening.

It is reasonable to assume that KDO in the capsular polysaccharides also interacts with divalent cations. KDO residues in the capsules of *Neisseria meningitidis* serogroup 29e (ref. 12) and *Escherichia coli* K6 (ref. 9), K12 (ref. 22), K13 (ref. 10), K14 (ref. 23), K2O (ref. 24), and K23 (ref. 25) are β. When the methyl β-glycoside of KDO (**3**) was allowed to interact with Mn^{2+} at the same concentrations as for **2** and **4** (Fig. 3), C-1 and C-8 were found to be mainly responsible for binding since their resonances and that of C-2 disappeared. Likewise, the resonances of C-1,2,8 disappeared when **1** interacted with Mn^{2+}. Also, the resonance for C-3 of **1** showed a larger downfield shift than that of C-3 for **3** (Fig. 4).

The involvement of the ring oxygen in the binding of metal ions by **2** and **4** was indicated by the complete disappearance of the signal for C-6 on the addition of Mn^{2+}. This signal was affected less in the spectra of **1** and **3** (Fig. 4).

Molecular models of **2** and **4** show a considerable concentration of the hydroxyl groups on the upper surface of the molecule, which creates a pocket into which the metal ion can fit. In the β-anomers **1** and **3**, the hydrophilic groups are not as concentrated on one side of the molecule as in the α anomers. According to these observations and the results of studies of the interaction of metal ions, it is assumed that the modes of binding of metal ions to α- and β-KDO are different.

REFERENCES

1 K. LUTHMAN, A. CLAESSON, K. GUSTAFSSON, AND G. BONDESSON, *Biochem. Biophys. Res. Commun.*, in press.
2 M. A. GHALAMBOR AND E. C. HEATH, *J. Biol. Chem.*, 241 (1966) 3216–3221.
3 P. H. RAY, C. D. BENEDICT, AND H. GRASMUK, *J. Bacteriol.*, 145 (1981) 1273–1280.
4 K. JANN, *ACS Symp. Ser. (Bacterial Polysaccharides)*, 231 (1983) 171–191.
5 H. BRADE, U. ZÄHRINGER, E. T. RIETSCHEL, R. CHRISTIAN, G. SCHULZ, AND F. M. UNGER, *Carbohydr. Res.*, 134 (1984) 157–166.
6 S. M. STRAIN, S. W. FESIK, AND I. M. ARMITAGE, *J. Biol. Chem.*, 258 (1983) 2906–2910.
7 R. CHRISTIAN, G. SCHULZ, P. WALDSTÄTTEN, AND F. M. UNGER, *Tetrahedron Lett.*, (1984) 3433–3437.
8 H. J. JENNINGS, R. ROY, AND R. E. WILLIAMS, *Carbohydr. Res.*, 129 (1984) 243–255.
9 H. J. JENNINGS, K.-G. ROSELL, AND K. G. JOHNSON, *Carbohydr. Res.*, 105 (1982) 45–56.
10 A. NESZMELYI, K. JANN, P. MESSNER, AND F. UNGER, *J. Chem. Soc., Chem. Commun.*, (1982) 1017–1019.
11 A. NESZMELYI, P. KOSMA, R. CHRISTIAN, G. SCHULZ, AND F. M. UNGER, *Carbohydr. Res.*, 139 (1985) 13–22.
12 A. K. BHATTACHARJEE, H. J. JENNINGS, AND C. P. KENNY, *Biochemistry*, 17 (1978) 645–651.
13 S. M. STRAIN, S. W. FESIK, AND I. M. ARMITAGE, *J. Biol. Chem.*, 258 (1983) 13466–13477.
14 K. LUTHMAN, M. ORBE, T. WÅGLUND, AND A. CLAESSON, *J. Org. Chem.*, in press.
15 P. MAIN, S. J. FISKE, S. E. HULL, L. LESSINGER, G. GERMAIN, J.-P. DECLERCQ, AND M. M. WOOLFSON, *MULTAN 80: A system of Computer Programs for the Automatic Solution of Crystal Structures from X-Ray Diffraction Data*, Department of Physics, University of York (Great Britain), 1980.
16 G. M. SHELDRICK, *SHELX 76: Program for Crystal Structure Determination*, University of Cambridge (Great Britain), 1976.
17 P. E. PFEFFER, K. M. VALENTINE, AND F. W. PARRISH, *J. Am. Chem. Soc.*, 101 (1979) 1265–1274.
18 D. CREMER AND J. A. POPLE, *J. Am. Chem. Soc.*, 97 (1975) 1354–1367.
19 F. M. UNGER, *Adv. Carbohydr. Chem. Biochem.*, 38 (1981) 323–388.
20 G. I. BIRNBAUM, R. ROY, J.-R. BRISSON, AND H. J. JENNINGS, *Int. Symp. Carbohydr. Chem., 13th, Ithaca 1986*, Abstr. B77.
21 M. E. DAMAN AND K. DILL, *Carbohydr. Res.*, 102 (1982) 47–57.
22 M. A. SCHMIDT AND K. JANN, *Eur. J. Biochem.*, 131 (1983) 509–517.
23 B. JANN, P. HOFMANN, AND K. JANN, *Carbohydr. Res.*, 120 (1983) 131–141.
24 W. F. VANN AND K. JANN, *Infect. Immun.*, 25 (1979) 85–92.
25 W. F. VANN, T. SODERSTROM, W. EGAN, F.-P. TSUI, R. SCHNEERSON, I. ØRSKOV, AND F. ØRSKOV, *Infect. Immun.*, 39 (1983) 623–629.